JOURNAL OF MATERIALS SCIENCE **39** (2004) 581 – 586

The oxidation of TiC in dry oxygen, wet oxygen, and water vapor

S. SHIMADA*, K. MOCHIDSUKI
Graduate School of Engineering, Hokkaido University, Sapporo 060-8628, Japan
E-mail: shimashi@eng.hokudai.ac.jp

Isothermal oxidation of TiC was studied using powder sample at 300–400°C in $Ar/O_2 =$ 95/5 kPa (dry oxidation) and $Ar/O_2/H_2O =$ 90/5/5–10 kPa (wet oxidation), and at 520–650°C in $Ar/H_2O =$ 95/5–15 kPa (H_2O oxidation) by monitoring weight changes. The phases produced were identified by X-ray analysis and the oxidized sample was observed by scanning and transmission electron microscopy. The dry, wet and H_2O oxidation of TiC was found to be described by a one-dimensional diffusion-controlling equation. It was revealed that the oxidation was divided into three steps, slow step I, fast step II, and slow step III. Water vapor in the wet oxidation accelerated these three steps, particularly step II. Non-isothermal oxidation of TiC was also performed to simultaneously monitor the evolved gases (CO/CO_2, H_2, CH_4) with weight changes by thermogravimetry and mass analysis. The accelerating effect of water vapor on oxidation of TiC was discussed from kinetic and thermoanalytical viewpoints. © *2004 Kluwer Academic Publishers*

1. Introduction

Titanium carbide (TiC) is high temperature structural material with very high melting temperature (>3000°C), high hardness, and high electrical conductivity. Many oxidation studies of TiC have been reported, most of which have been performed at various oxygen pressures from a kinetic viewpoint [1–4]. It is summarized that the oxidation of TiC powder or sintered pellet proceeds parabolically under intermediate oxygen pressure (P_{O_2}) (several to 100 kPa) and at temperatures of 600–800°C, in contrast to linear oxidation at high temperatures and oxygen pressures. One of the authors (S. S.) has studied the oxidation kinetics of TiC powder at relatively low temperatures of 350–500°C and demonstrated that the oxidation is described by a one-dimensional diffusion equation, consisting of four steps I–IV [4]. He also has investigated non-isothermal oxidation of TiC powder from simultaneous measurements of thermogravimetry (TG)—differential thermal analysis (DTA)—mass spectroscopy (MS), and confirmed four-stepped oxidation [5]. This non-isothermal TG-DTA-MS analysis was also applied to the oxidation of $Ti_{1-x}Ta_xC$ and $Ti_{1-x}Ta_x$ (C, N) whiskers and provided useful information on oxidation behaviors with varied compositions [6, 7].

The oxidation of TiC single crystal has also been investigated with the aim of examining the microstructure of oxide scale and revealing the interfacial reaction [8–10]. Reichle and Kickl studied the oxidation of crystals in O_2, an O_2/argon mixture, and CO_2/CO mixture at 800–1200°C [8]. Shimada *et al.* have performed the oxidation of crystals with the (200) face at 700–1500°C and $P_{O_2} = 0.08$–80 kPa, and showed that the oxide scale is composed of an inner dense lamella subscale with a carbon content of 7–23 at.% and an outer subscale and cracks [9]. Gozzi *et al.* have reported structural characterization of TiO_2 films formed by oxidation of crystals at an oxygen content of 180 ppm at 815°C [10].

As mentioned above, the oxidation of TiC has been performed under an atmosphere of O_2, O_2/argon, or CO_2/CO using both powder and crystal samples. It is well known that the oxidation of SiC and Si_3N_4 is accelerated under the presence of water through the dissolution of H_2O in SiO_2 scale [11–13]. Kiyono and Shimada have studied the dry and wet oxidation of β-Si_3N_4 and $Si_{6-z}Al_zO_zN_{8-z}$ (β-sialon) powders with $z = 1, 2, 3$ at various water vapor pressures [14, 15]. However, there has been no report on the wet oxidation of carbides except for SiC. It is of interest to investigate how water vapor in an O_2/H_2O atmosphere affects the oxidation kinetics of TiC and what kind of gases evolves during the oxidation of TiC in H_2O atmosphere. The present work is concerned with the oxidation kinetics of TiC powder under a flowing gas mixture of Ar/O_2 (dry oxidation), $Ar/O_2/H_2O$ (wet oxidation) and Ar/H_2O (H_2O oxidation) and discusses the effect of water partial pressure. MS analysis of gases evolved during the dry, wet and H_2O oxidation is also performed to complement the discussion about the effect of H_2O.

2. Experimental procedure

The starting material was the same commercially available TiC powder as used in previous reports [4, 5]. The

---

*Author to whom all correspondence should be addressed.

grains of TiC were of angular plate-like shape as observed by scanning electron microscopy (SEM). The grains had a mean size of about 2 μm with a relatively wide distribution. Weight changes of the TiC sample (about 20 mg) during oxidation were monitored by an electro-microbalance (Cahn Inc. D200). Isothermal oxidation was performed in the temperature range 300–650°C in Ar/O_2 (95/5 kPa) (dry oxidation), in $Ar/O_2/H_2O$ (90/5/5 and 85/5/10 kPa) (wet oxidation), and in Ar/H_2O (95/5, 90/10 and 85/15 kPa) (H_2O oxidation) under a flowing condition at 100 ml min^{-1}. The phases present in the samples after oxidation were identified by X-ray powder diffraction (XRD). Morphologies of TiC grains obtained by oxidation were observed by SEM and transmission electron microscopy (TEM). Gas analysis of CO_2, CO, H_2 and CH_4 was performed during the above oxidation by Q-Mass analysis (Fisons), with simultaneous measurements of weight change, for which the TiC sample was heated at a rate of 10°C min^{-1} to 1000°C.

3. Results and discussion

3.1. Dry and wet oxidation

Fig. 1 shows changes of the reacted fraction (α) with temperature (300–400°C) for over 80 h by the dry and wet oxidation under $Ar/O_2 = 95/5$ kPa and $Ar/O_2/H_2O = 90/5/5$ kPa. The α value was determined by dividing the measured weight gain by the theoretical one, which was calculated according to the Equation 1,

$$TiC + 2O_2 = TiO_2 + CO_2 \tag{1}$$

It is found that the oxidation of TiC is greatly accelerated in the presence of H_2O. For example, 100% oxidation was reached at 320°C for 15 h in the wet oxidation, while the temperature had to be increased to 400°C for the dry 100% oxidation. As a result of applying various rate equations, the oxidation in Fig. 1 was found to be best described by a one-dimensional diffusion-controlling equation as reported in a previous paper [4];

$$\alpha^2 = kt \tag{2}$$

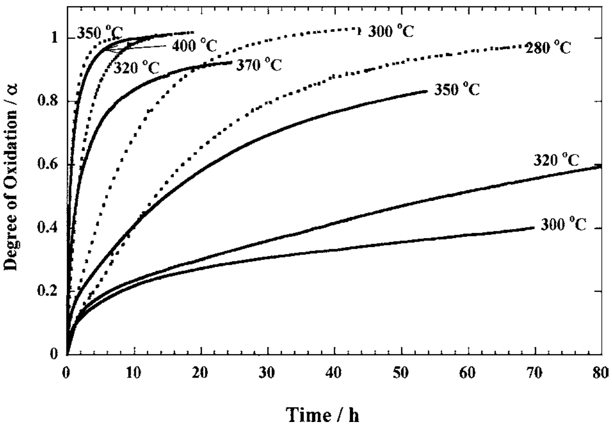

Figure 1 Isothermal oxidation of TiC in dry and wet oxygen. Dry oxidation (solid lines), $Ar/O_2 = 95/5$ kPa; wet oxidation (dashed lines), $Ar/O_2/H_2O = 90/5/5$ kPa.

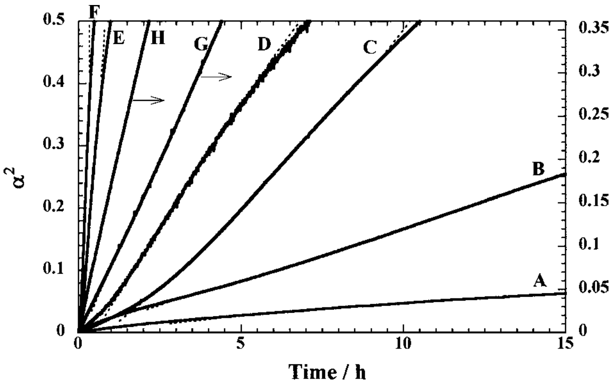

Figure 2 Plots of α^2 against t for the dry, wet, and H_2O oxidation. Curves A and B correspond to dry oxidation in $Ar/O_2 = 95/5$ kPa at 300 and 350°C, respectively; Curves C and D to wet oxidation in $Ar/O_2/H_2O = 90/5/5$ and 85/5/10 kPa, respectively, at 300°C; Curves E and F to wet oxidation in $Ar/O_2/H_2O = 90/5/5$ and 85/5/10 kPa, respectively, at 350°C; Curves G and H to H_2O oxidation in $Ar/H_2O = 95/5$ kPa at 550 and 600°C, respectively.

where k is the rate constant and t the time. Fig. 2 exemplifies the plots of α^2 versus t for the dry oxidation (300 and 350°C at $Ar/O_2 = 95/5$ kPa) and the wet oxidation (300 and 350°C at $Ar/O_2/H_2O = 90/5/5$ and 85/5/10 kPa). The kinetic plots give inflection points at $\alpha^2 = 0.04$–0.08 and above 0.4 for the dry and wet oxidation, as indicated by the dashed lines, implying that oxidation essentially consists of three steps, designated as I, II, and III. Step I is slow ($\alpha < 25\%$), step II fast ($25\% < \alpha < 65\%$), and step III slow ($\alpha > 65\%$). As reported in previous papers [4, 5], it is probable that the oxidation of TiC proceeds by a diffusion-controlled process involving oxygen. Although the oxidation of TiC is reported to consist of four steps, I (fast step), II (slow step), III (fast step), and IV (slow step), step I in this paper comprises both steps I and II in previous papers. This is probably because the step I was included in step II due to the slower rates, since the oxidation temperatures were lower in the present work than in the previously reported temperature range 400–500°C. To what extent the oxidation of TiC is accelerated by water vapor is realized from the ratio of the k_{wet} to k_{dry} in step II; the k_{wet} and k_{dry} are obtained from slopes for the plots of α^2 versus t in the dry and wet oxidation, respectively, in Fig. 2. The k_{wet}/k_{dry} was 17.5 and 25 at $P_{H_2O} = 5$ and 10 kPa, respectively, at 300°C, and 30 and 60 at $P_{H_2O} = 5$ and 10 kPa, respectively, at 350°C.

Non-isothermal oxidation in dry and wet atmospheres was performed by simultaneous TG-MS analysis to follow weight change and CO_2 evolution (Fig. 3). Oxidation begins at 320°C in both atmospheres, and is completed at 700 and 850°C in the wet and dry oxidation, respectively. From the TG curve, oxidation of TiC is divided into three steps, I to III, as shown by the dashed lines, in accordance with the isothermal oxidation; step I covers 0–25%, steps II 25–60%, and step III >65%. Three stepped CO_2 evolution is also observed, as judged from the three peaks I, II, and III. Although the wet oxidation does not give any distinct inflection on the TG curve, the CO_2 evolution takes place in three steps in almost the same temperature range as the dry oxidation. The wet oxidation containing 10 kPa H_2O

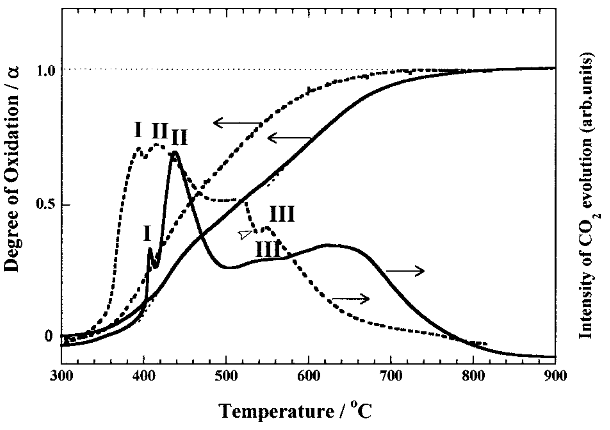

Figure 3 Simultaneous TG and CO_2 evolution curves by dry and wet oxidation. Dry oxidation (solid lines) in $Ar/O_2 = 95/5$ kPa and wet oxidation (dashed lines) in $Ar/O_2/H_2O = 90/5/5$ kPa. Heating rate, 10°C min^{-1}. A drop on the CO_2 evolution curve at 520–540°C by wet oxidation (see a small arrow) is due to mechanical events.

showed similar TG and CO_2 evolution behaviors. Neither CO nor H_2 nor CH_4 was detected. It is understood from TG-MS analysis that both dry and wet oxidation of TiC proceed in three steps covering $\alpha = 0$–25%, 25–60%, and >65%, in accordance with the three stepped isothermal oxidation.

Fig. 4 shows the XRD patterns of the sample obtained by both dry and wet oxidation at 320, 350, and 400°C. These samples gave 100% oxidation except for the dry oxidation at 320 and 350°C which gave $\alpha = 68$ and 83%, respectively. It is seen that the broad peaks from anatase appear with the sharp peaks of unreacted TiC in the dry oxidation at 320 and 350°C, in contrast to the wet oxidation which produces the relatively sharp anatase peaks. The dry 100% oxidation at 400°C produces only broad peaks of anatase, while a considerable amount of rutile is formed with anatase by the wet oxidation, suggesting that the transformation of anatase to rutile is promoted in an atmosphere containing H_2O.

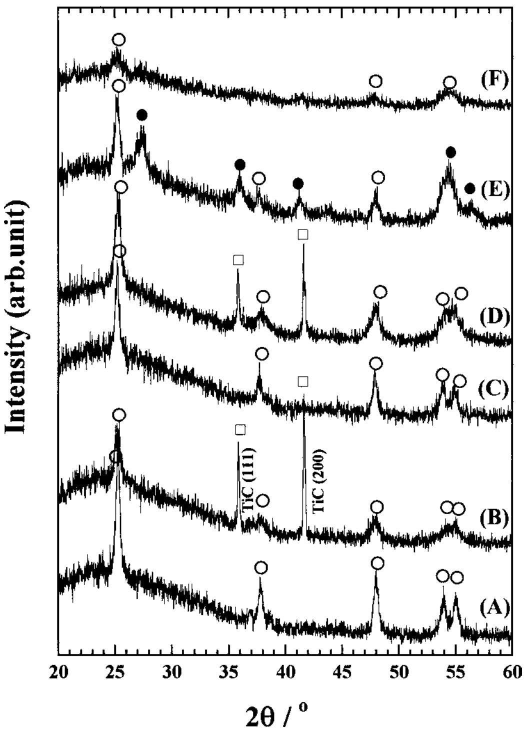

Figure 4 X-ray diffraction of the sample oxidized in dry and wet oxidation. (A) wet oxidation at 320°C, (B) dry oxidation at 320°C, (C) wet oxidation at 350°C, (D) dry oxidation at 350°C, (E) wet oxidation at 400°C, (F) dry oxidation at 400°C. Dry oxidation uses a mixture of $Ar/O_2 = 95/5$ kPa and wet oxidation that of $Ar/O_2/H_2O = 90/5/5$ kPa. ○ anatase, ● rutile, □ TiC.

It was observed by SEM of the dry oxidation samples that cracking does not occur at the fractions lower than 20%, but the grains crack along their edges at $\alpha = 30\%$. Therefore, the fast oxidation in step II is associated with cracking in the grains, providing fresh surfaces for further oxidation. TEM observation (Fig. 5A and B) shows that the 17%-oxidized sample at 350°C in $Ar/O_2/H_2O = 90/5/5$ kPa produces a continuous compact scale 10 nm thick with layered structure, while the 30%-oxidation produces agglomerates consisting of about 10 nm sized crystallite on cracked grains. Crystallites formed by the dry oxidation under the same condition were less than 10 nm sizes. Comparing the crystalline sizes obtained in the wet and dry oxidation, it is obvious that the presence of H_2O vapor promotes the grain growth of TiO_2. The compact layer formed in step I is responsible for the slow diffusion of oxygen. Agglomerates of nano-meter sized particles formed at $\alpha = 30\%$ should provide fast diffusion paths in step II.

Fig. 6 shows a relationship between the rate constants (k) in steps I and II and P_{H_2O} at 300°C in the wet oxidation. It is found that a linear and logarithm relation between k and P_{H_2O} is established in steps I and II, respectively; $k \propto P_{H_2O}$ in step I and $k \propto P_{H_2O}^{1/2}$ in step II. In step II, the accelerating effect of H_2O is saturated at $P_{H_2O} = 10$ kPa, above which the k values are not changed. It is suggested that water acts as H_2O and —OH in steps I and II, respectively; H_2O is adsorbed on the grains in step I and is dissolved in the TiO_2 scale in step II. The dissolved water reacts and exchanges with the TiO_2 network to form immobile —OH groups as Ti—OH (Equation 3);

$$1/2H_2O + \text{—TiO—} = \text{Ti—OH} \qquad (3)$$

The formation of these species may lead to deformation or disruption of the TiO_2 structure, which provides easy paths for the oxygen diffusion and/or enhances the movement of Ti^{4+} or O^{2-} ions, as being reflected by the slightly accelerated transformation of anatase to rutile with a slight grain growth. As illustrated in Fig. 7, the activation energy for the diffusion in step II in the dry oxidation was calculated to be about 200 kcal mol^{-1} and that for steps I and II in the wet oxidation to be almost the same (about 140 kcal mol^{-1}), independent of P_{H_2O} (5 and 10 kPa). The smaller activation energy in the wet oxidation might imply the easy oxygen diffusion paths.

3.2. H_2O oxidation

Fig. 8 shows the oxidation of TiC by H_2O in a temperature range 520–650°C. The H_2O oxidation occurs at higher temperatures than does the dry and wet oxidation. Oxidation exceeding 100% above 570°C occurs

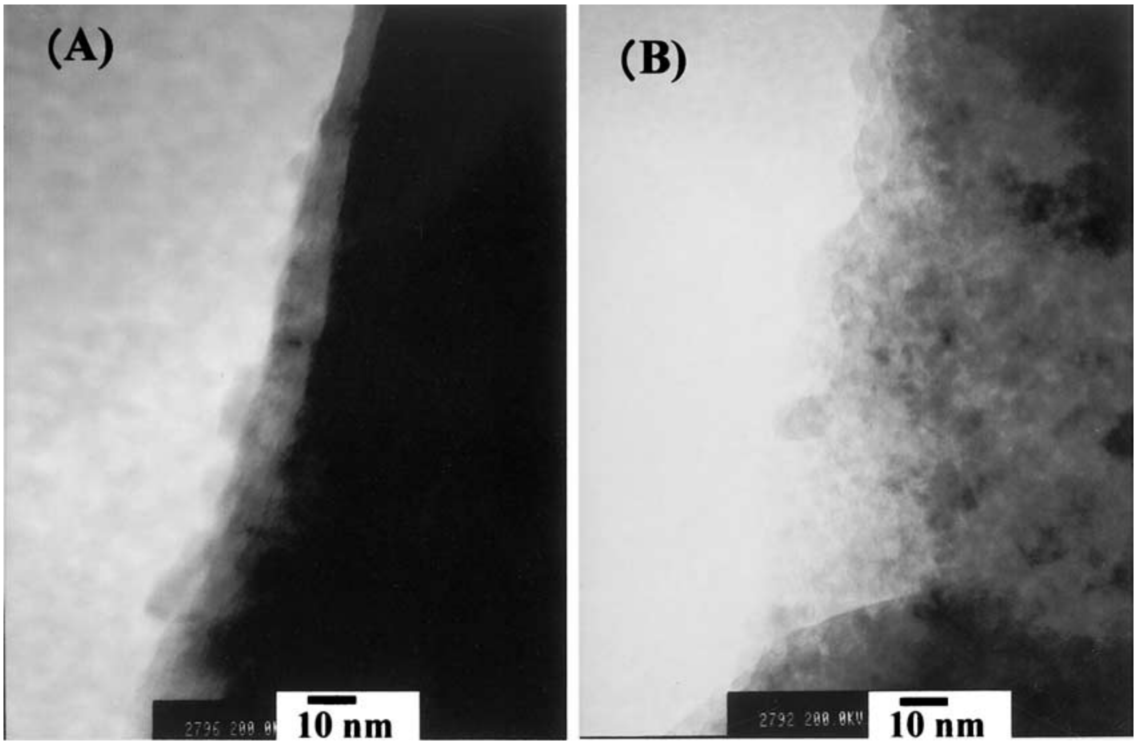

Figure 5 TEM photographs of the sample interrupted at 350°C in in $Ar/O_2/H_2O = 90/5/5$ kPa. (A) $\alpha = 17\%$ and (B) $\alpha = 30\%$.

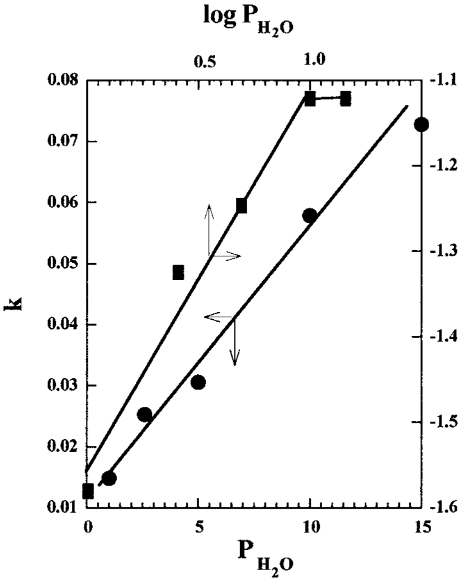

Figure 6 A relationship between k and P_{H_2O} for steps I and II in wet oxidation at 300°C. ● step I and ■ step II.

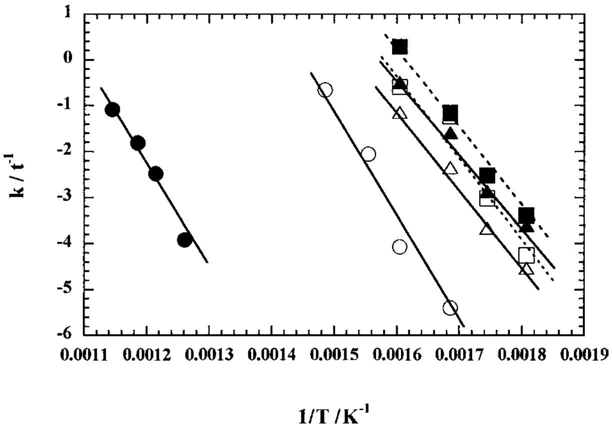

Figure 7 Arrhenius plots of rate constants versus reciprocal temperature. ○, dry oxidation ($Ar/O_2 = 95/5$ kPa); △, wet oxidation in step I ($Ar/O_2/H_2O = 90/5/5$ kPa, a solid line); ▲, wet oxidation in step II ($Ar/O_2/H_2O = 90/5/5$ kPa, a solid line); □, wet oxidation in step I ($Ar/O_2/H_2O = 85/5/10$ kPa, a dashed line); ■, wet oxidation in step II ($Ar/O_2/H_2O = 85/5/10$ kPa, a dashed line); ●, H_2O oxidation ($Ar/H_2O = 95/5$ kPa).

within 25 h, the extent of which increases with the maximum value shifting to lower temperature, as temperature is increased. Overshooting 100% oxidation is due to the retention of carbon, as explained below. It was found that the kinetics of the H_2O oxidation are also described by a one-dimensional diffusion-controlling equation (Equation 1), as shown by Fig. 2. The activation energy for step II in the wet oxidation was calculated to be about 180 kj mol^{-1} (Fig. 7). The sample completed to 100% oxidation produced only rutile at temperatures of >550°C, although both anatase and rutile were formed at 520°C. The H_2O oxidation produced well-crystallized rutile particles of about 50 nm size at 600°C.

Simultaneous TG and MS analysis for the H_2O oxidation of TiC at $Ar/H_2O = 95/5$ kPa (Fig. 9) shows that oxidation begins at 460°C, a much higher temperature than the dry and wet oxidation, overshoots 100% fraction at 820°C, passing on a maximum at 860°C, and is completed at 940°C. Overshooting 100% oxidation is attributed to the formation of carbon, as being supported by Raman spectra of the sample interrupted at 820°C, which showed two broad peaks at 1350 and 1600 cm^{-1} characteristic of existence of amorphous carbon. The formation of carbon should be associated with a low oxygen pressure at the reaction interface, which cannot oxidize the carbon component of TiC but oxidizes Ti [16]. The evolution of major H_2 and CO and minor

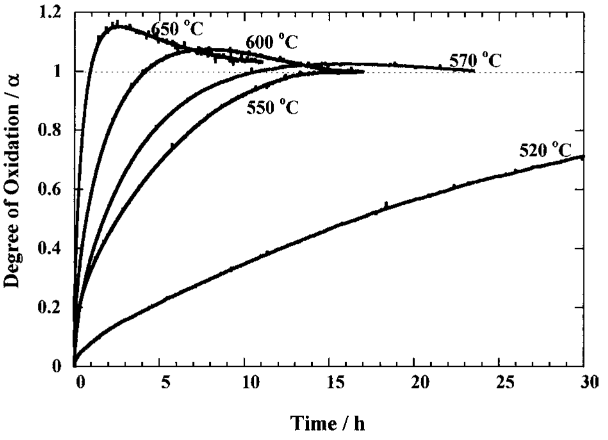

Figure 8 Isothermal oxidation of TiC by H_2O. $Ar/H_2O = 95/5$ kPa.

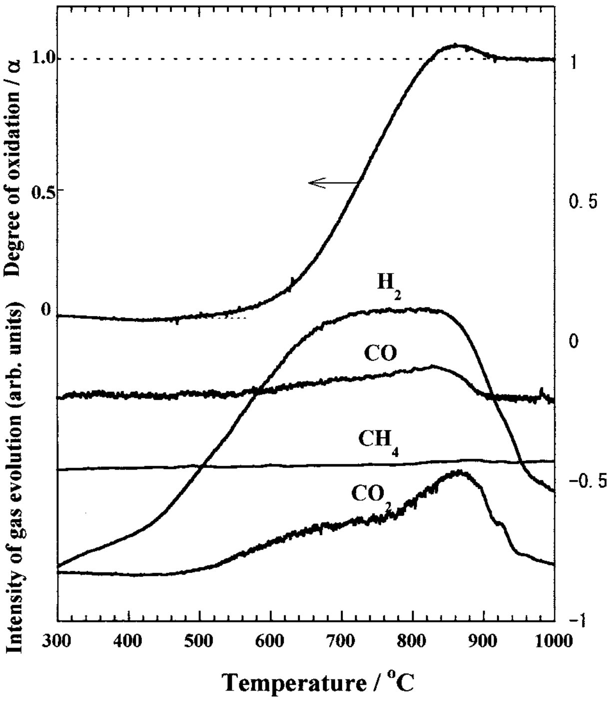

Figure 9 Simultaneous TG and MS analysis for H_2O oxidation of TiC. $Ar/O_2 = 95/5$ kPa. Heating rate = 10°C min^{-1}.

CO_2 is detected in a temperature range 500–940°C. These gas species and carbon are formed according to Equations 4 and 5;

$$TiC + 3H_2O \rightarrow TiO_2 + CO\,(CO_2) + 3H_2 \quad (4)$$

$$TiC + 2H_2O \rightarrow TiO_2 + 2H_2 + C \quad (5)$$

For simplicity, the first reaction is not balanced. H_2 is evolved from the very beginning of oxidation and continues to be generated over the whole temperature range. CO and CO_2 are increased with increasing temperature, particularly in the temperatures range 780–900°C. Thermodynamic calculations (Fig. 10) suggest that the formation of carbon with H_2 (Equation 5) prevails over the formation of CO (CO_2) with H_2 (Equation 4) below 740°C, since the ΔG° value for Equation 5 is negatively lower than that for Equation 4. The increased evolution of CO and CO_2 in a temperature range 780–900°C, in accordance with overshooting

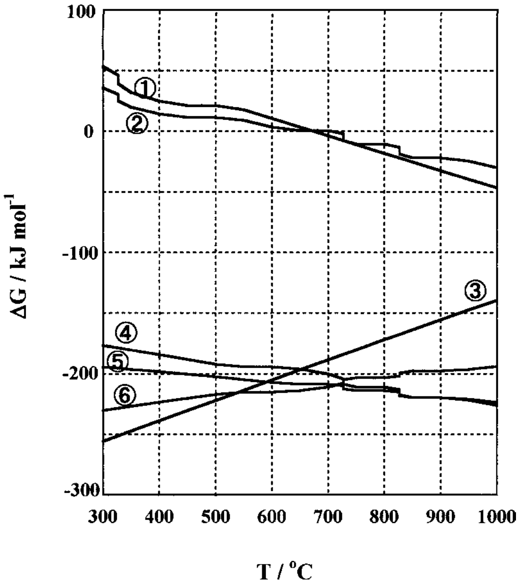

Figure 10 Equilibrium calculations for H_2O oxidation of TiC and C. ① $C + H_2O = CO + H_2$, ② $C + H_2O = CO_2 + H_2$, ③ $TiC + 2H_2O = TiO_2 + CH_4$, ④ $TiC + 3H_2O = TiO_2 + CO + 3H_2$, ⑤ $TiC + 4H_2O = TiO_2 + CO_2 + 4H_2$, ⑥ $TiC + 2H_2O = TiO_2 + C + 2H_2$. Reflections on the lines ①, ②, ④, ⑤, ⑥ at 330, 730, and 830°C are due to the use of thermodynamic data from the different sources [17].

100% oxidation, is due to the H_2O oxidation of carbon remaining unreacted in the sample. The formation of carbon should occur at <740°C. Therefore, the oxidation of C with H_2O proceeds (Equation 6) in parallel with the reactions of Equations 4 and 5;

$$C + H_2O = CO\,(CO) + H_2 \quad (6)$$

Thermodynamic calculations also suggest that the reaction of Equation 6 should occur above 680°C. Since H_2O acts as an oxidant against TiC at >500°C from Fig. 9, it seems unlikely that H_2O in the wet oxidation at lower temperatures <350°C participates in direct oxidation of TiC.

4. Conclusion

Isothermal oxidation of TiC was performed using a powder sample at 300–400°C in $Ar/O_2 = 95/5$ kPa (dry oxidation) and in $Ar/O_2/H_2O = 90/5/5–10$ kPa (wet oxidation) and at 520–650°C in $Ar/H_2O = 95/5–15$ kPa (H_2O oxidation). The oxidation was best described by the one-dimensional diffusion-controlling equation; $\alpha^2 = kt$. It was found that the oxidation was divided into three steps, slow step I ($\alpha < 25\%$), fast step II ($25\% < \alpha < 65\%$), and slow step III ($\alpha > 65\%$). Water vapor in the wet oxidation accelerated these steps, particularly step II, and promotes the transformation of anatase to rutile with slightly enhanced grain growth. It was suggested from the dependence of water vapor pressure on the k values that water diffuses as H_2O and —OH in steps I and II, respectively. The main gas evolved during oxidation was CO_2 in both dry and wet oxidation, whereas H_2 and CO/CO_2 were formed in the H_2O oxidation. In the H_2O oxidation, carbon was retained in oxidized sample. The activation energy for the diffusion was obtained to be about 200 and 140 kcal mol^{-1} in the dry and wet oxidation, respectively, and 180 kcal mol^{-1} in the H_2O oxidation.

References

1. Y. A. LAVRENKO, L. A. GLEBOV, A. P. POMITKIN, V. G. CHUPRINA and T. G. PROTSENKO, *Oxid. Metals* **9** (1975) 171.
2. R. W. STEWART and I. B. CUTLER, *J. Amer. Ceram. Soc.* **50** (1967) 176.
3. B. O. HAGLUND and B. LEHTINEN, in “Thermal Analysis,” in Proceeding of the Third ICTA, Davos (197) Vol. 3, p. 545.
4. S. SHIMADA and M. KOZEKI, *J. Mater. Sci.* **27** (1992) 1869.
5. S. SHIMADA, *ibid.* **31** (1996) 673.
6. M. JOHNSSON and S. SHIMADA, *J. Mater. Sci. Lett.* **21** (2002) 955.
7. S. SHIMADA, Y. SEKI and M. JOHNSSON, *Solid State Ionics* (accepted).
8. M. REICHLE and J. J. NICKL, *J. Less-Common Metals* **27** (1972) 213.
9. S. SHIMADA, F. YUNAZAR and S. OTANI, *J. Amer. Ceram. Soc.* **83** (2000) 721.
10. A. BELLUCCI, F. DI. PASCASIOI, D. GOZZI, S. LORETI and C. MINARINI, *Thin Solid Films* **405** (2002) 1.
11. N. S. JACOBSON, *J. Amer. Ceram. Soc.* **76** (1993) 3.
12. E. J. OPILA and R. E. HANN, Jr, *ibid.* **80** (1997) 197.
13. E. J. OPILA, *ibid.* **82** (1999) 625.
14. H. KIYONO and S. SHIMADA, *J. Electrochem. Soc.* **148** (2001) B79.
15. H. KIYONO, S. SHIMADA and K. J. D. MACKENZIE, *ibid.* **148** (2001) 86.
16. S. SHIMADA, *J. Ceram. Soc. Jpn.* **109** (2001) S33.
17. GTT-CHEMSAGE (version 4.01), GTT-Tecnnologies, Acchen, Germany, 1998.

Received 2 October 2002
and accepted 25 August 2003